Green Chemistry

PAPER

View Article Online
View Journal | View Issue

Cite this: *Green Chem.*, 2024, **26**, 5194

Eco-foaming lignin for innovative rigid foam†

Qiangu Yan,[a] Timothy Ketelboeter,[a] Wenjun Fan,[b] Caixia Wan *[b] and Zhiyong Cai*[a]

Received 26th December 2023,
Accepted 19th February 2024

DOI: 10.1039/d3gc05123d

rsc.li/greenchem

Rigid lignin foam is prepared by a baking method using kraft lignin as the sole source. The eco-forming process involved cold-pressing kraft lignin powder into a solid block, heating the solid block to form lignin foam, and finally curing and cooling the lignin foam to obtain an open-cell, rigid foam. Both adsorbed water and water generated from the dehydration of hydroxyl groups in the lignin served as the blowing agent in this baking method. It was found that as the moisture content of lignin decreased, the foam densities increased, the mean bubble sizes decreased, and the bubble size distributions became narrower. Foam morphology showed an open cell structure and a wide cell volume distribution. The results suggest that controlling the moisture content in raw lignin allows for the control of the pore structure of the lignin foam. Based on their unique properties, lignin foam materials hold great promise in many applications especially as core insulation materials for structural insulated panels (SIPs).

1. Introduction

Lignin, a major component of lignocellulosic biomass and the most abundant naturally occurring aromatic polymer, has been reported as being used in making foam composites for insulation materials. Such foam materials serve as green alternatives to replace counterparts based on petrochemicals (mainly polystyrene (PS)) or inorganics (*e.g.*, glass wool).[1] In addition to insulation, rigid foam boards also provide structural strength, increase thermal break, provide exterior sheathing, and serve as an air barrier.[1,2] If successfully exploited, lignin-based foam could open huge market opportunities for technical lignin. Approximately 70 million metric tons of technical lignin are produced annually worldwide,[3] and cost-effective utilization of lignin is an integral part of lignin valorization to ensure profitable pulping and biorefinery industries. There are several problems to be addressed in developing lignin-based foam. Traditionally, lignin formulated into rigid foam is used either as a reactant in the formation of foam, such as in polyurethane foam, or as a filler to increase mechanical strength. Typically, lignin-containing rigid foam contains as high as 37% lignin.[4] Such lignin-derived foam products may not be either eco-manufactured or fully biodegradable. Thus, we have been motivated to develop fully lignin-based foam (so-called lignofoam) *via* a baking method. This is a non-catalytic, single-step foaming process proven effective for making open-cell rigid foam with great promise for structural insulated panels (SIPs) as core materials. In our previous study,[5] we fabricated carbon foam with high mechanical strength, excellent thermal conductivity, and superb fire resistance *via* simultaneous lignin foaming and carbonization at a temperature of 400–600 °C under atmospheric pressure followed by further carbonization/graphitization at an elevated temperature of 700–1000 °C under an inert atmosphere. Although this process involved lignin foaming *via* baking, lignin experienced carbonization during both stages. Lignin foaming at relatively low temperatures for noncarbonized foam products has not been reported so far. Moreover, foaming mechanisms have not been studied in depth, fundamental factors controlling foaming have not been well identified, and no guidance is available for the rational design of lignofoam.

The main objective of this work was to investigate the role played by moisture/water in foaming of lignin. Moisture was found to play a key role in determining the foam cell structure and mechanical properties. The foam synthesized under optimal conditions showed excellent structural and mechanical properties and good thermal insulation properties for SIP applications. This work provides useful guidance for manufacturing lignin-based foam materials and improving their performance.

[a]*Forest Products Laboratory, USDA Forest Service, One Gifford Pinchot Drive, Madison, WI 53726-2398, USA. E-mail: zhiyong.cai@usda.gov; Tel: +1 608-231-9446*
[b]*Department of Chemical and Biomedical Engineering, University of Missouri, 1406 East Rollins Street, Columbia, MO 65211, USA. E-mail: wanca@missouri.edu; Tel: +1 573 884 7882*

† Electronic supplementary information (ESI) available. See DOI: https://doi.org/10.1039/d3gc05123d

2. Materials and methods

2.1. Lignin feedstock

Kraft lignin (BioChoice®, Plymouth, NC, USA) was supplied by Domtar Corporation. As received, this kraft lignin contained

28–35 wt% water. The lignin was first dried in air at room temperature and labeled as KL25 with 7.4% moisture. The air-dried lignin (KL25) was further dried at 50, 75, 100, 125, and 150 °C to reach the respective moisture levels of 4.5%, 2.2%, 1.4%, 0.5%, and 0% (Table S1†), denoted as KL50, KL75, KL100, KL125, and KL150, respectively.

2.2. Preparation of lignin foam (LF)

A process for the fabrication of lignin foam from kraft lignin has been developed and consists of two main steps (Scheme 1): (1) cold-pressing lignin powder into a solid block and (2) foaming of the lignin block. Three hundred grams of kraft lignin was placed into a kitchen blender and crushed for 2 minutes. The lignin powder was then transferred to a mold as detailed in our previous studies.[6] A metal plate was placed in the mold on the top of the lignin powder and lignin was cold-pressed under a pressure of up to 650 psi. The mold containing the pressed lignin block was transferred to a Thermo Scientific Heratherm OMH750 advanced lab oven (Thermo Electron LED GmbH, Langenselbold, Germany). The oven was then heated at a rate of 10 °C min^{-1} to 240 °C and held for 60 minutes. After baking, the mold was allowed to cool down naturally to room temperature. This process resulted in the formation of open-cell lignin foam. The foam samples prepared using kraft lignin dried at their respective temperatures were denoted as LF25, LF50, LF75, LF100, LF125, and LF150.

2.3. Characterization

Moisture contents of lignin samples were analyzed following the ASTM E871 method using a Mettler Toledo HE73 moisture analyzer. The attenuated total reflectance Fourier transform infrared spectroscopy (ATR-FTIR) spectra were acquired on a Thermo Scientific ATR-FTIR spectrometer (Thermo Scientific, Nicolet iZ10) at a resolution of 4 cm^{-1} for 64 scans in the 500 to 4000 cm^{-1} range. The thermal properties of the samples were analyzed using a Mettler-Toledo TGA/DSC3+ system (Mettler-Toledo, LLC. Columbus, OH, USA). Scanning electron microscopy (SEM) images were acquired on a Zeiss EVO 50 scanning electron microscope (Jena, Germany). Pore size distribution, porosity, and average pore size of the lignin foam samples (LF25–LF125) were analyzed based on SEM images using ImageJ software. The compressive strength of lignin foam was analyzed following ASTM C365[7] using an INSTRON 5869 mechanical testing machine, and the foam samples were cut into 25.4 × 25.4 × 12.5 mm pieces for testing. Thermal insulation properties of lignin foam were measured using a Hot Disk TPS 1500 thermal constants analyzer (ThermTest, Fredericton, NB, Canada) following the ISO/DIS 22007-2.2 standard method.[8]

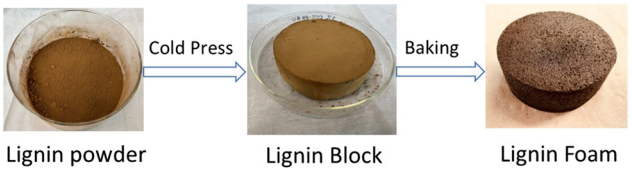

Scheme 1 Fabrication process of foam from kraft lignin.

3. Results and discussion

3.1. Structural changes in lignin during steam-induced foaming

Since the lignin foaming process is mainly caused by steam, the FTIR bands related to adsorbed water and hydroxyl groups in kraft lignin are of most interest. There are 7 bands at 3700–3000 cm^{-1} related to adsorbed water and –OH groups (Table S3†) in addition to common absorption bands in FTIR spectrum of kraft lignin (Table S2 and Fig. S1†). The bands at 3602.5 and 3555.2 cm^{-1} correspond to weakly hydrogen-bonded water and weakly adsorbed water, respectively.[9] Other –OH-related bands are observed at 3496.0 cm^{-1} (valence vibration of hydrogen-bonded –OH groups or moderately hydrogen-bonded water), 3372.8 cm^{-1} (intramolecular hydrogen-bonded –OH stretching), 3280.2 cm^{-1} (–OH intramolecular and intermolecular stretching modes), and 3149.5 cm^{-1} (strongly hydrogen-bonded water). Besides the bands at 3700–3000 cm^{-1}, the band at 1652.3 cm^{-1} is also related to –OH vibration (*i.e.*, –OH bending in adsorbed water and –OH bending affected by water adsorption).[10] To compare the changes of –OH-related bands under different treatment conditions, the band at 1511.5 cm^{-1} (aromatic skeleton stretching vibrations) is selected as a reference since it represents the strongest and most stable functional group in the lignin structure.[11,12]

We first studied the effects of moisture content on the structural changes of lignin samples during foaming. The FTIR spectra of kraft lignin samples with different moisture contents are shown in Fig. 1a. The intensity ratios of adsorbed water and –OH group bands to the band of the aromatic skeleton (1511.5 cm^{-1}) are calculated, normalized, and plotted in Fig. 1b. This shows that the samples with decreasing moisture content from 7.4% to 0.5% resulted in decreasing band intensities of adsorbed water and –OH groups in kraft lignin. The intensities of the bands related to the adsorbed water (3602.5, 3555.2, and 1652.3 cm^{-1}) were attenuated faster than those of the bands assigned to hydroxyl groups (3496.0, 3372.8, 3280.2, and 3149.5 cm^{-1}). With the decrease in moisture content (from 7.4% to 0.5%), the band intensities reduced in the order of $I_{3602.5} > I_{3555.2} > I_{1652.3} > I_{3149.5} > I_{3280.2} > I_{3372.8} > I_{3496.0}$, indicating that chemically bonded hydroxyl groups are relatively stable compared to adsorbed water.

TG, DTG, and DSC curves for the kraft lignin powder dried under different temperatures are shown in Fig. 2. The TG/DTG curves obtained for kraft lignin show two-stage weight loss in the study temperature range (30–240 °C). The first stage (30–130 °C) is characterized by a mass loss due to evaporation of adsorbed moisture, with the peak temperatures of 70–82 °C for lignin samples with different moisture content. The second weight loss stage (130–240 °C) is mainly attributed to the dehydration of chemically bonded water and hydroxyl groups in

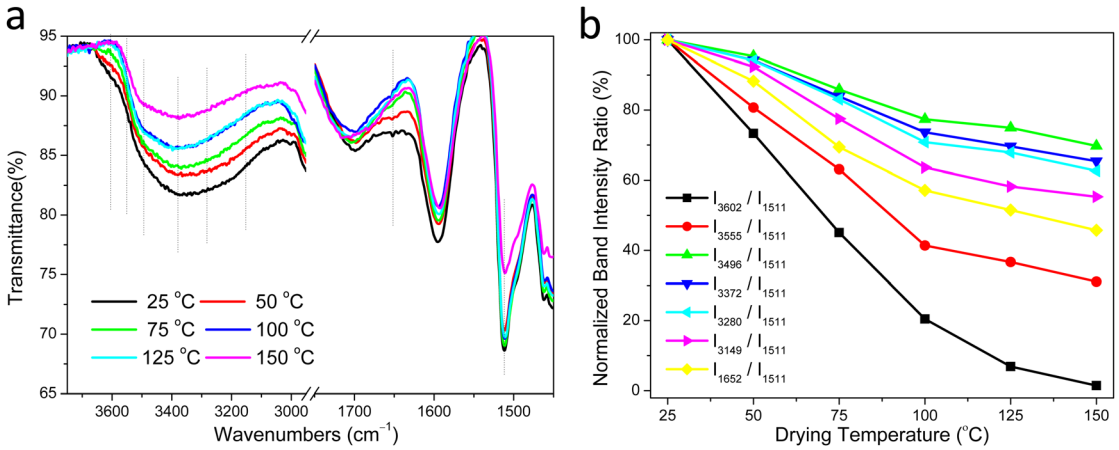

Fig. 1 FTIR spectra (a) and the water and hydroxyl group-related band intensity ratios (b) of kraft lignin samples dried at different temperatures.

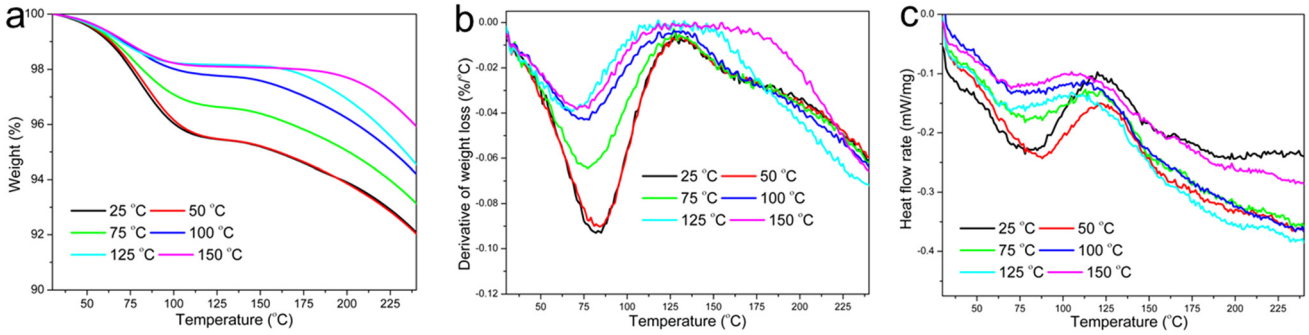

Fig. 2 Thermal properties of kraft lignin dried at different temperatures: (a) TG, (b) DTG, and (c) DSC curves.

lignin. According to the FTIR results, the band associated with hydroxyl groups was attenuated significantly due to dehydration reactions when lignin was heated to 200 °C and higher,[13] while other functional groups remained unchanged. It was found that in Fig. 2a and b that the TGA/DTG curves of four lignin samples with a moisture content of 2.2% or above (KL25–KL100) show very similar thermal behaviors, while the KL125 and KL150 samples demonstrate different TG/DTG plots between 130 and 240 °C. Due to little or no moisture content, the KL125 and KL150 samples may undergo partial dehydration reactions under drying conditions. Furthermore, KL150 (with no moisture) was dried above the glass transition temperature of kraft lignin (T_g = ~145 °C),[14] which led to changes in both the thermal properties and structure of kraft lignin.

The DSC curves for kraft lignin samples also show two-stage heat flow in the temperature range of 30–240 °C (Fig. 2c). The first stage (30–130 °C) is characterized by an endothermic heat flow due to evaporation of adsorbed moisture. The second heat absorbing stage (130–240 °C) is mainly attributed to the dehydration of chemically bonded water and hydroxyl groups in lignin.

The effects of cold-press pressure (0–500 psi) on the structural changes of lignin were studied using KL25. Cold-pressing pressure did not significantly change lignin chemistry since the intensity ratios of the selected band to that of the aromatic skeleton band (1511.5 cm^{-1}) remained constant across different pressing pressures (Fig. 3a and b).[11] The TG/DTG curves show three stages of weight loss (Fig. 4a and b). The first stage of weight loss from 30–130 °C was due to evaporation of adsorbed moisture. Water vapor was transported through dense materials mainly by the differential pressure across the solid body. The water vapor pressure gradient was affected by factors like porosity, geometry, size, complexity of pores, pore shape, and pore size distribution.[15] It was observed that the peak temperature of this stage increased with increasing cold-press pressure, starting at 76.2 °C for 0 psi (no pressing), 80.0 °C for 75 psi, 85.8 °C for 150 psi, 86.9 °C for 300 psi, and 91.1 °C for 500 psi. This shift in the peak is due to higher press pressures leading to more compact lignin solids with fewer and smaller pores or tunnels for the transport of moisture in the more densified lignin block. The adsorbed water remained in the compact lignin block even when heating the sample over the boiling point of water. For the sample pressed at 500 psi, the evaporation of the adsorbed water continued above 150 °C. Weight loss during heating also decreased with increasing pressing pressure, further proving that the densified sample helped trap moisture during the baking process.

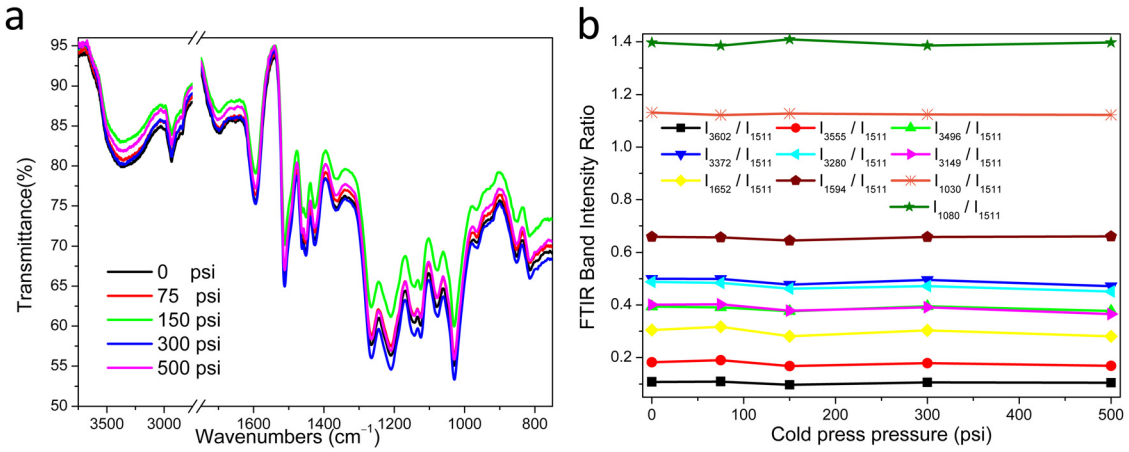

Fig. 3 FTIR spectra (a) and the water and hydroxyl group-related band intensity ratios (b) of kraft lignin samples cold-pressed at different pressures.

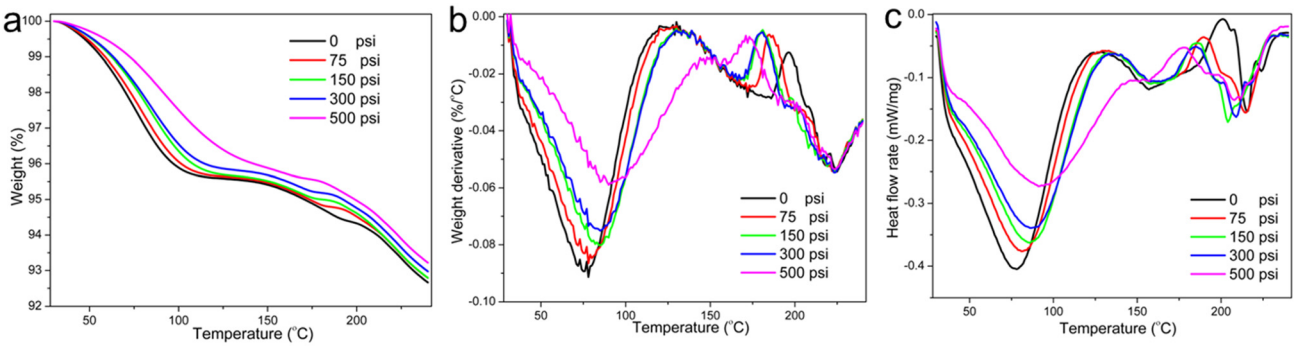

Fig. 4 Thermal properties of kraft lignin samples cold-pressed at different pressures: (a) TG, (b) DTG, and (c) DSC curves.

The second weight loss stage (130–195 °C) was mainly attributed to the dehydration of chemically bonded water and hydroxyl groups in lignin. DTG curves (Fig. 4b) show that the weight loss peaks become narrower and shift to lower temperatures with increasing cold-press pressure. As the dominant functional group, hydroxyl groups can be categorized into phenolic and aliphatic hydroxyl groups. Dehydration reactions between these hydroxyl groups in lignin can occur intra- and inter-molecularly. The dehydration of hydroxyl groups is affected by several factors such as the types, the density, the location of hydroxyl groups in the molecule, and the distance between the adjacent hydroxyl groups. Fig. 4b shows no obvious weight loss peaks between 130 and 195 °C for the loose lignin powder samples, indicating that the dehydration reaction is promoted in the pressed samples since the density of hydroxyl groups is increased. The increased density decreases the distance between the hydroxyl groups and lowers the activation energy, allowing –OH groups to dehydrate more easily and shift the dehydration to lower temperatures. The dehydration reaction may mainly occur intramolecularly, with minor intermolecular reactions in loose or less densified samples, while the reaction in the adequately pressed lignin samples may have a comparatively higher intermolecular reaction component. Due to the prevalent dehydration of the pressed lignin at 130–195 °C, a considerable amount of water can be formed as steam. This high steam level helps decrease the softening temperature of lignin.[16] Decreasing the softening temperature allowed more steam to be trapped, resulting in less water loss from the lignin matrix. The third weight loss stage (195–240 °C) is mainly attributed to the dehydration of hydroxyl groups in lignin and the release of trapped steam bubbles in the softened lignin matrix. With increasing baking temperature from 195 to 240 °C, more hydroxyl groups are dehydrated to form steam, causing the steam bubbles in the softened lignin to continue expanding. When the steam pressure in the bubbles is high enough, it will break through the softened lignin body and generate a foam structure with interconnected gas channels.

The sample loading also affects structural changes. The higher the sample loading was, the smaller the resulting heat and mass transfer areas were.[1] Moisture transfer distance also increased with the increase in sample loading. Therefore, it is obvious that increasing the sample loading decreased the moisture transport and evaporation rate as reflected by the shift of weight loss peaks associated with moisture evaporation to higher temperatures in DTG curves (Fig. S2†). However,

sample loading did not affect the –OH group dehydration temperature in lignin.

3.2. Characteristics of lignin foam

Table 1 lists the densities and compressive strength of the lignin foam samples prepared from kraft lignin cold-pressed at 150 psi. The bulk densities of the foam samples (LF25, LF50, LF75, LF100, LF125, and LF150) are 0.21, 0.25, 0.27, 0.30, 0.37 and 0.83 g cm^{-3}, respectively. It is obvious that decreasing lignin moisture content led to an increase in the foam density. Lower moisture content results in less steam trapped in the softened lignin. Less blowing agent (steam) obstructs the expansion of lignin to create a less porous structure, therefore, the bulk density of lignin foam increases with decreased moisture content. For the sample dried at 150 °C (KL150), all adsorbed moisture evaporated, and the hydroxyl groups partially dehydrated, leading to a non-foamed product with a bulk density of 0.83 g cm^{-3}, similar to that of the pressed lignin block (0.85–0.88 g cm^{-3}).

SEM images of lignin foam samples are shown in Fig. 5 and Fig. S3.† The foam samples exhibited open-cell structures. The pores were interconnected because the expanding steam bubbles in the softened lignin ruptured the thin walls between the bubbles. LF125 had the most uniform porous structure with the smallest average pore size (152.2 μm) among all the five samples (Fig. 5e). In contrast, LF50, LF75 and LF100 showed less uniform pore distributions with smaller sizes (Fig. 5b–d). Their respective average pore sizes were 345.6, 342.1, and 237.4 μm (Fig. 6). When the foam was made of lignin with further increased (LF25) or reduced (LF150) moisture (7.4% and 0%, respectively), the porous structures were not desirable. LF25 showed a nonuniform porous structure with a wide range of pore sizes ranging from 100 to over 1000 μm (Fig. 5a and 6), whereas LF150 was still solid, with no pore structures formed (Fig. 5f). The porosity and pore size distribution might be predominantly controlled by the adsorbed water in lignin, which acts as the major source of the blowing agent during foaming, for making the LF25, LF50, and LF75 foam samples. Both the adsorbed and dehydrated water acted as the blowing agent for LF100. Water resulting from dehydration served as the major blowing agent for LF125. The porosity of lignin foam decreased with decreasing moisture content in the feedstock. Low moisture content yields fewer and smaller steam bubbles in the softened lignin, which results in lower porosity of the foam products. This agrees with the trend of foam densities (Table 1).

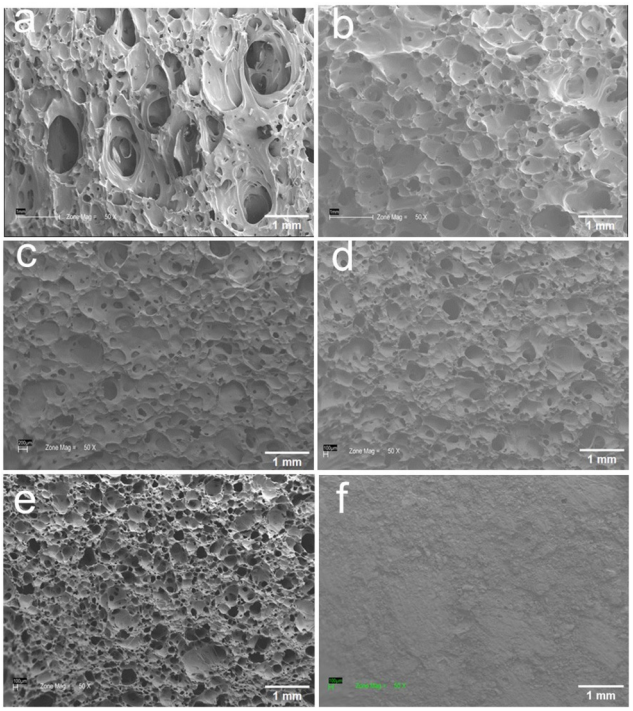

Fig. 5 SEM images of lignin foam specimens under 50× magnification: (a) LF25, (b) LF50, (c) LF75, (d) LF100, (e) LF125, and (f) LF150.

The mechanical properties of lignin foam materials depend on the initial precursor compositions, densities of the foam materials, and microstructural arrangement in the foam materials.[17] The compressive strengths of the foam samples (LF25, LF50, LF75, LF100, LF125, and LF150) are measured as 1.18, 1.51, 1.62, 1.87, 2.47 and 6.36 MPa, respectively (Table 1). The compressive strengths of the lignin foam samples increase with decreasing lignin moisture content because this strength is proportional to the density. Young's modulus showed a similar trend to compressive strength and increased from 25.2 to 54.8 MPa when the moisture content of lignin for foaming decreased from 7.4% to 0.5%. Foam samples with lower densities exhibit higher porosity but lower compressive strength and Young's modulus.[18] Compared to commercial foam pro-

Table 1 Characteristics of lignin foam samples

Lignin foam	Porosity (%)	Average pore size (μm)	Density (g cm^{-3})	Compressive strength (MPa)	Young's modulus (MPa)	Thermal conductivity (W m^{-1} K^{-1})
LF25	94.0	347.2	0.21 ± 0.03	1.18 ± 0.16	25.2 ± 1.7	0.030 ± 0.003
LF50	90.9	345.6	0.25 ± 0.02	1.51 ± 0.13	35.6 ± 2.5	0.035 ± 0.002
LF75	87.8	342.1	0.27 ± 0.02	1.62 ± 0.15	36.2 ± 2.3	0.038 ± 0.003
LF100	83.4	237.4	0.30 ± 0.02	1.87 ± 0.18	40.3 ± 3.6	0.043 ± 0.003
LF125	81.2	152.2	0.37 ± 0.03	2.47 ± 0.21	54.8 ± 4.9	0.052 ± 0.004
LF150	N/A	N/A	0.83 ± 0.03	6.36 ± 0.19	120.5 ± 8.2	0.081 ± 0.002

N/A: no pores.

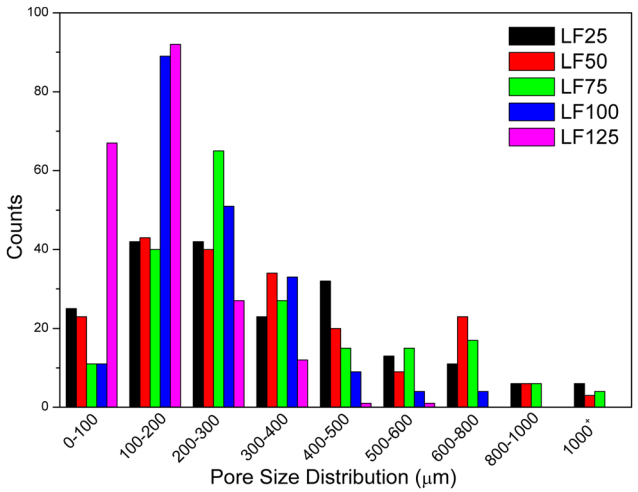

Fig. 6 Pore size distribution in lignin foam samples prepared from kraft lignin dried at different temperatures.

ducts, the density and compressive strength of the lignin foam samples are also higher than those of commercial polystyrene (PS) foam[19] and are comparable to the phenolic-based polyurethane (PU) foam[20] (Table S4†). Moreover, the foam samples showed good thermal insulation properties (Table 1 and Table S4†). The lower the foam density is, the better its thermal insulation is (Fig. S4†). Thermal conductivities as low as 0.030 W m^{-1} K^{-1} were obtained from LF25. With its relatively uniform pore structure, LF125 also showed a lower thermal conductivity (0.043 W m^{-1} K^{-1}).

Since the lignin foam has good thermal insulation properties and high compressive strengths that are comparable to or even better than commercial petrochemical-based foam materials (Table S4†), it shows great promise as a structural insulated panel (SIP) core material, yielding an SIP building material that is potentially carbon negative. The manufacturing process was scaled up to make large size (LF75) lignin foam (Fig. 7a). These lignin foam panels were used as composite cores for structural insulated panels (SIPs) with a dimension of 16″ wide × 64″ long × 4″ thick (Fig. 7b). This prototyping for scaled-up production is a critical step to go beyond the proof of concept and toward commercialization. In the future work, the lignin-based SIP will be investigated for building performance and code requirements.

3.3. Possible mechanisms for lignin foaming and stabilization

To create a cellular structure, a blowing agent must be used during the foaming process.[21] Blowing agents can be categorized into physical blowing agents (PBAs) and chemical blowing agents (CBAs) based on the origin of gas for foaming.[22] In the lignin foaming process of this work, water vapor is the proposed blowing agent. Prior studies also reported using water as both a blowing agent and plasticizer of starch-based foam in a baking process.[23] During the preparation of starch-based foam, when the temperature is higher than the boiling point of water, some of the water contained in the starch-based materials becomes gaseous and creates bubbles. The remaining water acts as a plasticizer to gelatinize the starch and provide melting strength, enabling the expansion of the starch-based materials to form a foam structure. It was reported that water is adsorbed by van der Waals bonds or by electrostatic forces over wood-based polymers when the moisture content is over 6%, and the adsorbed moisture forms a multi-molecular water layer which results in non-uniform distribution of water in wood, lignin, or cellulose.[24] This non-uniform distribution of water can explain the non-uniform pore size distribution observed in the LF25 foam, which had greater than 6% moisture content. When the moisture content is below 6%, water molecules are interacted by H-bonds of functional groups in cellulose or lignin, forming a mono-molecular layer.[24] Therefore, water molecules in lignin containing less than 6% moisture content could be more evenly distributed among functional groups in lignin when its moisture content is reduced. This could explain the more uniform pore

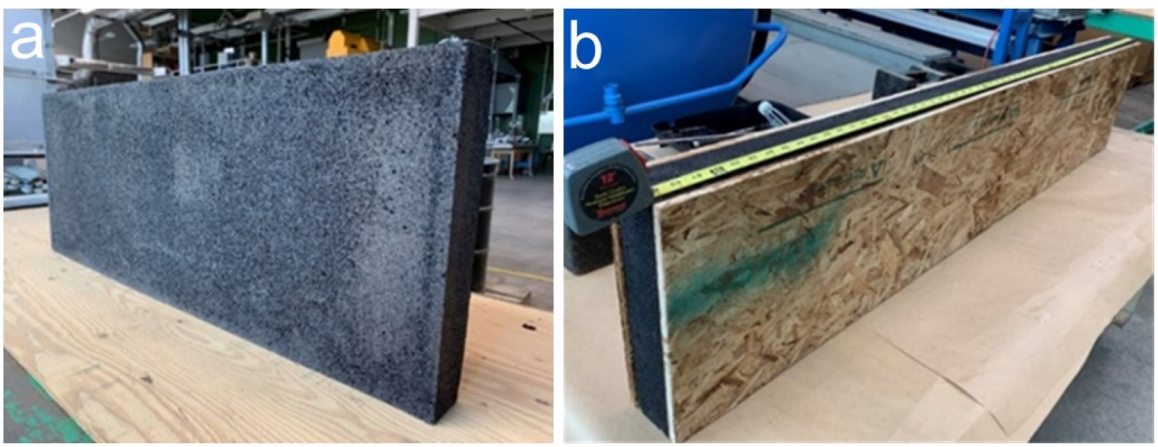

Fig. 7 (a) A lignin foam sample with dimensions of 16″ wide × 36″ long × 5″ thick. (b) A finished SIP sample with the lignin foam core (16″ wide × 64″ long × 4″ thick).

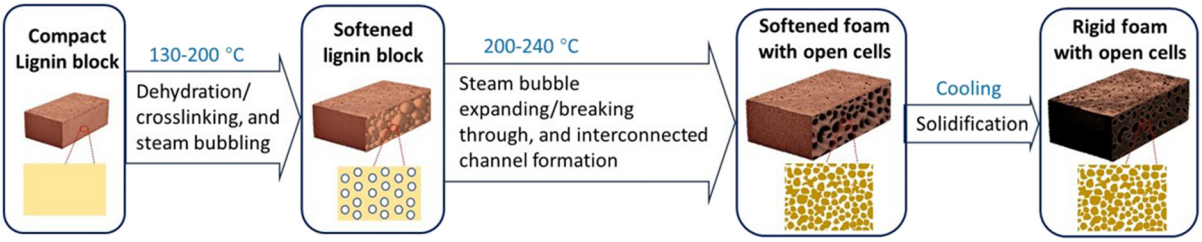

Scheme 2 Possible foaming mechanism of kraft lignin by a baking process.

size and pore size distribution of the lignin foam samples when water was reduced to a lower and optimal level.

Lignin is composed of an aromatic skeleton containing numerous functional groups like hydroxyl (both phenolic and aliphatic), methoxyl, carbonyl, and carboxyl groups. These functional groups are hydrophilic and act as adsorption sites by forming hydrogen bonds with water, allowing lignin to adsorb water molecules.[25] The physiochemical properties of lignin are significantly affected by its moisture content.[26] In this work, it is proposed to foam kraft lignin using the adsorbed water as the blowing agent through a thermal process. Softening temperatures of lignin range from 127 to 193 °C;[27] however, kraft lignin will not soften and melt until the tempreture reaches 150 °C or higher.[28] Thus, it is very important to trap water vapor in lignin until lignin softens or melts. The factors influencing gas diffusion include porosity, bulk density, diffusing gas species, and aggregate size of the matrix.[29] To trap moisture while increasing the temperature, we thus compressed lignin into a compact lignin block at room temperature. This compact lignin block had high bulk density and low porosity, which restricted the movement of gas and water in the confined dense lignin block. When heating compact lignin at an elevated temperature, significant water vapor should be trapped until the lignin reaches its softening or melting temperature. The trapped water vapor serves as a blowing agent to bubble and foam the softened/melting lignin.

Besides the adsorbed water, which can serve as a physical blowing agent for lignin feedstock, another water resource may be generated by dehydration reactions between two adjacent –OH groups in lignin. Dehydration reactions of lignin usually occur in the temperature range of 100–200 °C, while cross-linking/condensation reactions simultaneously occur to form large molecules. Water from the dehydration reaction of –OH groups is a type of chemical blowing agent in the lignin foaming process. Dehydration can occur during the cross-linking/polymerization of lignin molecules, first by the heat-generating auto-polymerization between lignin molecules and later by the reaction of free –OH groups of lignin molecules under thermal conditions.[30] The foaming or bubble formation inside lignin foam is caused by vaporizing either the moisture adsorbed in lignin, or the water generated through dehydration/cross-linking reactions.

Based on the role of water in lignin foaming discussed above, we propose the possible foaming mechanism illustrated in Scheme 2. There are three major stages involved in foaming. First, the compact lignin matrix swells when heated from room temperature to 130 °C[31] and the physically adsorbed moisture diffuses inside the lignin matrix as shown in TGA and DSC results (Fig. 2 and 4). Then, upon further increasing the baking temperature from 130 to 200 °C, the lignin block undergoes the softening/melting process, and the adsorbed moisture vaporizes and creates steam vesicles inside the softened lignin matrix.[24] Some adjacent hydroxyl groups in lignin are dehydrated, releasing water that joins the adsorbed water in the steam vesicles in the softened lignin matrix (supported by TGA and FTIR results). Intra- and inter-molecular cross-linking/condensation reactions simultaneously occur between lignin molecules, furthering the polymerization process of kraft lignin. In the final stage, upon further increasing the heating temperature from 200 to 240 °C, more hydroxyl groups are dehydrated to form steam. This causes the steam bubbles in the softened lignin to continue expanding while the viscosity of the melted/softened lignin decreases. The bubbles break through the lignin matrix when the steam pressure in the bubbles is high enough (DSC data, Fig. 2), resulting in a softened lignin foam with interconnected gas channels. With continuous polymerization caused by dehydration/cross-linking reactions, more high molecular weight fractions are formed during the foaming process, causing an increase in the viscosity of the lignin block and initializing solidification of the lignin foam. Rigid lignin foam with an open cell structure is achieved when the foamed lignin matrix is cooled to room temperature.

4. Conclusions

Rigid foam samples were prepared from kraft lignin as the sole source through baking-based eco-foaming. The lignin foam precursors are first compressed into a lignin block in a mold, then the lignin block is heated to generate a lignin foam in the temperature range of 200–240 °C. The foam samples had the density of 0.21–0.37 g cm^{-3}, the porosity of 81–94%, the average pore size of 152.2–347.2 μm, the compressive strength of 1.18–6.36 MPa, and the thermal conductivity of 0.035–0.048 W m^{-1} K^{-1}. The moisture content in the feedstock can be used to control the pore structure of the lignin foam. With decreasing moisture content from 7.4% to 0.5%, the pore structure

becomes more uniform. The average pore sizes could be predominantly controlled by the origin of the steam blowing agent. Adsorbed moisture (7.4–2.2%) could be the major source of the steam blowing agent during the foaming process. Water resulting from dehydration could contribute to foaming when the initial moisture is further reduced and even act as the major blowing agent when there is little intitial moisture. Based on impressive thermal insulation property and high compressive strength, the lignin foam materials have many potential applications such as core insulation materials of structural insulated panels (SIPs).

Conflicts of interest

There are no conflicts to declare.

Acknowledgements

This work was supported by the USDA Forest Service through Grant No. 19-JV-11111124-053, 19-JV-11111124-063, and 20-JV-11111124-035, and Wood Innovations (Grant No. 20-DG-11094200-234). The authors would like to thank Domtar Corporation for providing kraft lignin. Special thanks to Joseph Destree, Joshua Limbaugh, Kimberly Hoxie, CR Boardman, Sara J. Fishwild, Marshall M. Begel, and Will Kinney at the USDA Forest Products Laboratory, for their help in making this project run successfully.

References

1 F. Asdrubali, F. D'Alessandro and S. Schiavoni, *Sustainable Mater. Technol.*, 2015, **4**, 1–17.
2 J. A. Charlson, *US Pat.*, 6125608A, 2000.
3 D. Bajwa, G. Pourhashem, A. H. Ullah and S. Bajwa, *Ind. Crops Prod.*, 2019, **139**, 111526.
4 V. Mimini, V. Kabrelian, K. Fackler, H. Hettegger, A. Potthast and T. Rosenau, *Holzforschung*, 2018, **73**, 117–130.
5 Q. Yan, R. Arango, J. Li and Z. Cai, *Mater. Des.*, 2021, **201**, 109460.
6 Z. Cai, Q. Yan and J. Li, *US Pat.*, 11142458B2, 2021.
7 ASTM-C578-23, *Standard Specification for Rigid*, *Cellular Polystyrene Thermal Insulation*, 2023.
8 ISO22007-2, *Determination of thermal conductivity and thermal diffusivity*, 2022.
9 M. Báder, R. Németh, J. Sandak and A. Sandak, *Cellulose*, 2020, **27**, 6811–6829.
10 M. Kačuráková, P. S. Belton, R. H. Wilson, J. Hirsch and A. Ebringerová, *J. Sci. Food Agric.*, 1998, **77**, 38–44.
11 O. Faix, *Holzforschung*, 1991, **45**, 21–28.
12 X. Guo, Y. Wu and N. Yan, *Wood Sci. Technol.*, 2018, **52**, 971–985.
13 N. Mahmood, Z. Yuan, J. Schmidt and C. C. Xu, *Bioresour. Technol.*, 2013, **139**, 13–20.
14 H. Jeong, J. Park, S. Kim, J. Lee, N. Ahn and H. Roh, *Fibers Polym.*, 2013, **14**, 1082–1093.
15 M. Lawrence and Y. Jiang, *Bio-aggregates based building materials: state-of-the-art report of the RILEM technical committee 236-BBM*, 2017.
16 W. Cousins, *Wood Sci. Technol.*, 1976, **10**, 9–17.
17 S. Li, Y. Song, Y. Song, J. Shi, L. Liu, X. Wei and Q. Guo, *Carbon*, 2007, **45**, 2092–2097.
18 X. Meng, J. Xu, J. Zhu, Z. Li, J. Zhao, M. J. Reece and F. Gao, *J. Am. Ceram. Soc.*, 2020, **103**, 6088–6095.
19 L. Ravindran, M. Sreekala, S. Anilkumar and S. Thomas, *Thermal Stability of Phenolic Foams*, 2022.
20 Q. Xu, R. Gong, M. Cui, C. Liu and R. Li, *High Perform. Polym.*, 2015, **27**, 852–867.
21 W. Yamsaengsung and N. Sombatsompop, *Composites, Part B*, 2009, **40**, 594–600.
22 G. Coste, C. Negrell and S. Caillol, *Eur. Polym. J.*, 2020, **140**, 110029.
23 L. Meng, H. Liu, L. Yu, Q. Duan, L. Chen, F. Liu, Z. Shao, K. Shi and X. Lin, *Ind. Crops Prod.*, 2019, **134**, 43–49.
24 I. Hartley, F. Kamke and H. Peemoeller, *Wood Sci. Technol.*, 1992, **26**, 83–99.
25 Z. Gao, Y. Ding, W. Yang and W. Han, *J. Mol. Model.*, 2017, **23**, 1–19.
26 N. Volkova, V. Ibrahim, R. Hatti-Kaul and L. Wadsö, *Carbohydr. Polym.*, 2012, **87**, 1817–1821.
27 D. Goring, *Consolidation of the Paper Web*, 1965, vol. 1, pp. 555–575.
28 H. Jeong, J. Park, S. Kim, J. Lee and J. W. Cho, *Fibers Polym.*, 2012, **13**, 1310–1318.
29 A. R. Grable and E. Siemer, *Soil Sci. Soc. Am. J.*, 1968, **32**, 180–186.
30 T. Varila, H. Romar, T. Luukkonen, T. Hilli and U. Lassi, *Heliyon*, 2020, **6**, e03228.
31 B. Jiang, C. Chen, Z. Liang, S. He, Y. Kuang, J. Song, R. Mi, G. Chen, M. Jiao and L. Hu, *Adv. Funct. Mater.*, 2020, **30**, 1906307.